JOURNAL OF GEOPHYSICAL RESEARCH, VOL. 113, D18114, doi:10.1029/2008JD009920, 2008

Different ENSO teleconnections and their effects on the stratospheric polar vortex

C. I. Garfinkel[1] and D. L. Hartmann[1]

Received 5 February 2008; revised 19 May 2008; accepted 26 June 2008; published 30 September 2008.

[1] Reanalysis data are used to study the El Niño–Southern Oscillation (ENSO) signal in the troposphere and stratosphere during the late fall to midwinter period. Warm ENSO events have extratropical tropospheric teleconnections that increase the wave 1 eddies and reduce the wave 2 eddies, as compared to cold ENSO. The increase in wave 1 overwhelms the decrease in wave 2, so the net effect is a weakened vortex. This modification in tropospheric wave forcing is induced by a deepening of the wintertime Aleutian low via the Pacific–North America pattern (PNA). Model results are also used to verify that the PNA is the primary mechanism through which ENSO modulates the vortex. During easterly Quasi-Biennial Oscillation (EQBO), warm ENSO does not show a PNA response in the observational record. Consequently, the polar vortex does not show a strong response to the different phases of ENSO under EQBO, nor to the different phases of QBO under WENSO. It is not clear whether the lack of a PNA response to warm ENSO during EQBO is a real physical phenomenon or a feature of the limited data record we have.

Citation: Garfinkel, C. I., and D. L. Hartmann (2008), Different ENSO teleconnections and their effects on the stratospheric polar vortex, *J. Geophys. Res.*, *113*, D18114, doi:10.1029/2008JD009920.

1. Introduction

[2] Over the past few years, ENSO has been shown to have a significant effect on the Northern Hemisphere winter polar vortex. *Brönnimann et al.* [2004] found that El Niño affects the lower stratospheric polar vortex, and thus modifies Europe's wintertime climate. *Sassi et al.* [2004] forced a General Circulation Model (GCM) with observed sea surface temperatures (SSTs) from 1950 to 2000 and found that while the warm phase of ENSO (WENSO) leads to a significantly warmer polar stratosphere, the cold phase of ENSO (CENSO) is statistically indistinguishable from the mean. The effect was more pronounced in late winter to early spring. *Manzini et al.* [2006] and *Garcia-Herrera et al.* [2006] compared model results forced with observed SSTs and ERA-40 data from 1980 to 1999, and they found that while WENSO winters were significantly warmer than neutral ENSO months in the Arctic stratosphere, the CENSO cooling was weaker; *Manzini et al.* [2006] found that the signal propagated downward over the course of winter, such that the upper stratospheric signal was most pronounced in early winter and the lower stratospheric effect strongest in late winter. *Taguchi and Hartmann* [2006] forced a GCM with perpetual January conditions under both WENSO and CENSO SST conditions in the Pacific, and found more Sudden Stratospheric Warmings and a more disturbed vortex under WENSO than CENSO conditions. *Brönnimann et al.* [2006] compared reanalysis data to a chemistry climate model in a case study; over Europe and the lower stratosphere, the different sources of data agreed, but over the midstratosphere, differences emerged. *Camp and Tung* [2007] applied Linear Discriminant Analysis to observational data to show that the ENSO signal is of comparable magnitude to that of the QBO. *Garfinkel and Hartmann* [2007] (hereinafter referred to GH07) and *Brönnimann* [2007] found that in observational data, the polar stratosphere was significantly warmer in WENSO winters than CENSO winters under WQBO conditions but not under EQBO conditions. It is now well established that ENSO affects the polar vortex.

[3] Several of the aforementioned papers show an anomalous EP flux convergence in the polar region in WENSO, which must accompany the warming of the polar region. But the physical mechanism that connects ENSO to the polar vortex remains unclear. *Manzini et al.* [2006] linked the WENSO-induced PNA pattern to an increase in wave 1 at the polar vortex, but *Baldwin and O'Sullivan* [1995] (hereinafter referred to as BO95) found that the three patterns associated with ENSO, the PNA, WP (western Pacific), and TNH (tropical Northern Hemisphere) patterns, do not affect the polar vortex. In particular, BO95 found that the PNA does enhance wave 1 in the troposphere, but the signal does not propagate into the stratosphere. Thus, three questions remain:

[4] 1. How does WENSO set up this increased wave 1? Is the warmer vortex related to an ENSO-induced tropospheric extratropical pattern?

[1]Department of Atmospheric Science, University of Washington, Seattle, Washington, USA.

0148-0227/08/2008JD009920$09.00

[5] 2. Why is the difference between CENSO and WENSO so much smaller under EQBO than under WQBO?

[6] 3. *Taguchi and Hartmann* [2006] found that more (less) wave 1 (wave 2) EP flux propagates upward from the troposphere under WENSO as compared to CENSO. How important is the wave 2 decrease?

[7] The proximate cause of the wave 1 response to ENSO, and the peculiar effect of EQBO (questions 1 and 2), will be addressed in sections 4 and 5, respectively. The relative importance of wave 1 and wave 2 is examined throughout. Section 6 confirms the results of section 4 using WACCM (Whole Atmosphere Community Climate Model) data.

[8] In addition to the effect of ENSO on the polar stratosphere, studies dating back to *Holton and Tan* [1980] have noted that the vortex is less disturbed during the westerly phase of the QBO at 50 hPa than during the easterly phase. Recently, GH07 and *Wei et al.* [2007] found that in observational data, the vortex is weaker in EQBO as compared to WQBO under CENSO and neutral ENSO but not under WENSO. A last question concerns the disappearance of the QBO effect under WENSO. Does the warming of the pole "saturate," or is something external to the QBO's ability to affect the polar vortex obscuring the conventional QBO effect? The answer to this question will be discussed in section 5.2.

2. Data

[9] The 1200 UTC data produced by the European Center for Medium-Range Weather Forecasts (ECMWF) is used. The ERA-40 data set is used for the first 45 years [*Uppala et al.*, 2005], and the analysis is extended by using operational ECMWF TOGA analysis. All relevant data from the period September 1957 to August 2007 are included in this analysis, yielding 50 years of data. The extended winter season of NDJF (November/December/January/February) is examined except in section 5.2, where ONDJ (October/November/December/January) is examined. Following GH07, we use a NDJF composite in order to maximize the size of the composite while still only including months where a similar response to ENSO is expected. Differences between months within the extended winter season are not examined because of the shortness of the observational record.

[10] The ENSO index used is the Nino 3 index from the CPC/NCEP (http://www.cpc.noaa.gov/data/indices/sstoi.indices). The CPC/NCEP indices for the PNA, WP, and TNH patterns are used as well. They are computed by a rotated principal component analysis of the monthly mean 500 hPa heights from 1950 to 2000 [*Barnston and Livezey*, 1987]. For brevity, the noun "pattern(s)" will be dropped henceforth when describing the PNA, WP, and TNH. See http://www.cpc.ncep.noaa.gov/data/teledoc/teleindcalc.shtml for more details. The QBO index used is the zonal mean, 10°S–10°N area averaged zonal wind from the ECMWF data at 50 hPa. All indices were normalized by their standard deviation over all 594 months from September 1957 to February 2007. A month is considered to be a QBO, ENSO, PNA, WP, or TNH month if the QBO/ENSO/PNA/WP/TNH index exceeds a certain fraction of a standard deviation from its mean value. Except where indicated, this fraction is 0.6 standard deviations.

[11] As defined by the CPC, the PNA and WP have positive correlations with ENSO, and the TNH has a negative correlation with ENSO. In the rest of this paper, the phase of PNA that is associated with WENSO is denoted WPNA, and the phase of PNA associated with CENSO is denoted CPNA. Similarly, the phase of WP (TNH) associated with WENSO is denoted WWP(WTNH), and the phase of WP(TNH) associated with CENSO is denoted CWP(CTNH). This convention is used even in section 4 where we examine PNA and WP events that occur when the ENSO index is near neutral. The PNA can be excited independently of ENSO [*Simmons et al.*, 1983]. The canonical extratropical pattern associated with anomalous ENSO convection closely resembles the PNA (*Horel and Wallace* [1981], *Hoskins and Karoly* [1981], and summarized by *Trenberth et al.* [1998]), though the exact spatial signature of the PNA and ENSO may not be identical [*DeWeaver and Nigam*, 2002; *Hoerling et al.*, 1997]. By using the language of PNA, WPO, and TNH, we explore how the details of the extratropical response to ENSO affects the stratosphere.

[12] We do not exclude presatellite era data, as this did not seem to have much of an effect on the results in GH07. The ECMWF data are available on pressure levels, and are converted to log-pressure heights using a scale height of 7 km. Finally, our graphs extend to the 1 hPa level. ERA-40 is increasingly inaccurate above the 10 hPa level [*Randel et al.*, 2004]. Thus, results above this level should be taken with a grain of salt.

3. Diagnostic Tools Used

[13] Four different types of figures are included. They are EP flux diagrams, cross sections of the variance of the geopotential height at a particular zonal wavenumber, the longitudinal structure of geopotential height on a given pressure level, and the polar cap geopotential as a function of height. Composites of variables are created in the different phases of ENSO, ENSO's teleconnections, and the QBO. The significance of the difference between two appropriately chosen composites is evaluated for three of these variables.

[14] An example of an EP flux diagram is Figure 2 (see section 4.2). These diagrams are produced as follows. The anomaly from the zonal mean for u, T, ω and v of the daily ECMWF data is taken. The zonal Fourier cross spectrum between v' and u', u' and ω', and v' and θ' are computed, and the real part of the wave 1 and wave 2 components are stored. In addition, $\overline{v'\theta'}$, $\overline{\omega'u'}$, and $\overline{v'u'}$ are computed. These covariances are then used to compute the EP flux vectors using the equations that are given by *Vallis* [2006, p. 537] and *Andrews et al.* [1987, p. 128]. The spherical geometry, primitive equation form of the EP flux is used. A monthly average of the EP flux is computed for each month. The annual cycle is computed by averaging over each calendar month, and the annual cycle is then subtracted from the raw EP fluxes to produce the anomalous EP fluxes. Once composites are produced of the anomalous EP fluxes during the different phases of ENSO and QBO, a Monte Carlo test is used to establish significance. If either component of the

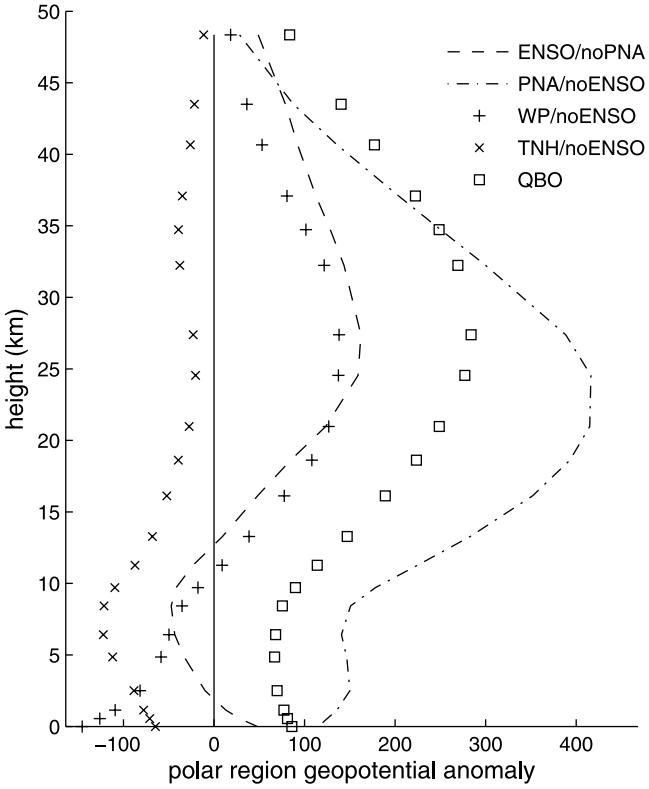

Figure 1. The difference in area averaged geopotential anomaly from 70°N and poleward between WENSO/noPNA and CENSO/noPNA, WPNA/noENSO and CPNA/noENSO, WWP/noENSO and CWP/noENSO, EQBO and WQBO, and WTNH/noENSO and CTNH/noENSO months. A month is included in the composite if its index exceeds 0.6. The only significant region is the PNA/noENSO from 37 km all the way to 13 km and the QBO over the entire stratosphere. The height has been multiplied by $\rho_0^{\frac{1}{2}}$, the square root of the basic state density, in order to ease viewing in the troposphere.

EP flux is significantly different between the two phases, the point is shaded gray.

[15] The Monte Carlo test for the difference between WPNA and CPNA under noENSO is performed as follows (the test for the other comparisons is identical). Two groups of months are randomly selected without repetition from NDJF over all 50 years, with the size of each group equal to the number of degrees of freedom in the WPNA/noENSO and CPNA/noENSO composites, respectively. To account for the autocorrelation from month to month, we reduce the number of degrees of freedom for the WPNA/noENSO and CPNA/noENSO composites from the number of months; specifically, if 3 or 4 months occur consecutively, 2 degrees of freedom are assigned, and if 2 months occur consecutively, 1 degree of freedom is assigned. The average EP flux in each of these groups is evaluated, and then the difference between the two groups at each point in latitude and height is computed. 5000 such random pairs of months are taken, and the difference between all 5000 pairs is stored. The observed difference between WPNA and CPNA under noENSO is compared to these 5000 pairs by evaluating the percentage of the 5000 random pairs that have a smaller EP flux difference than the EP flux difference between WPNA and CPNA. If the percentage is greater than 97.5 or less than 2.5, the point in latitude/height space is deemed to have significantly more (or less) EP flux.

[16] The divergence of the EP flux is computed in units of m s^{-1} d^{-1}, not as a torque like in the work by *Dunkerton et al.* [1981]. The zero contour is omitted. To produce plots of the EP flux vectors such that one can visually predict where convergence and divergence will occur, the vectors need to be scaled. We scale them by the ratio of $\frac{1}{r_0 \cos\phi}\frac{\partial}{\partial\phi}$ to $\frac{\partial}{\partial z}$. Thus, the ratio of $F^{(\phi)}$ to $F^{(z)}$ is the average distance between adjacent vertical levels in the ECMWF data between 500 hPa and 5 hPa (2.5 km), divided by the radius of the Earth times the average angular displacement between adjacent latitudes (278 km). Since our plots are approximately square, the plotted vectors should appear divergent when they are. (*Dunkerton et al.* [1981] use log-p coordinates and also have a similar aspect ratio of degrees latitude to height. Via a completely different argument, they arrive at the ratio $\frac{.05 r_0}{5.559}$ =.008994 r_0 = 5.72*e*4. But the extra factor of r_0 arises because they plot the EP flux capable of generating a torque on the zonal circulation, so our ratio of .0087 is almost the same as their .00899.)

[17] EP flux arrows in the stratosphere are rescaled so as to be visible. Similar to *Naito and Yoden* [2006], arrow lengths are multiplied by a factor of 5 above 100 hPa. A reference arrow for the stratosphere is located in the top left hand corner of the plot; its vertical component is $1.0879 \times 10^5\ kgs^{-2}$, and its horizontal component is $1.25 \times 10^7\ kgs^{-2}$. The title of the graph contains the number of months making up the composite. The 1 hPa and 1000 hPa levels are excluded.

[18] We also plot the difference of the wave variance of ϕ between different phases of ENSO, ENSO's teleconnections, and the QBO. The power spectrum is the decomposition by wavenumber of the total variance; thus, a plot of the wave 1 or wave 2 component of the power spectrum shows the variance explained by a given wavenumber. The wave variance, rather than the actual amplitude (like in BO95), is plotted because of the relationship between the total variance of the stream function and the EP flux for Rossby waves on a β plane with constant static stability and uniform zonal flow [e.g., *Vallis*, 2006, p. 300; *Andrews et al.*, 1987, p. 188].

[19] Like the EP flux, the wave variance is computed from the daily ECMWF data, averaged into monthly means, and then has the climatology removed. The wave variance is multiplied by the density before plotting. After composites are produced for the various phases of ENSO and QBO, a Monte Carlo test identical to that used for EP fluxes is used to test for significance. The only difference is that light gray and dark gray correspond to significantly positive and negative regions, respectively. An example of this type of figure is Figure 5 (right) (see section 4.2).

[20] We also plot the anomalous pattern of geopotential height on a given pressure level on the left side of figures like Figure 6 (see section 5.1). Above each plot is the average normalized ENSO index for the months in the composite (positive values are WENSO), the average (non-normalized) QBO index for the months in the composite (positive values are WQBO), and the number of months in the composite.

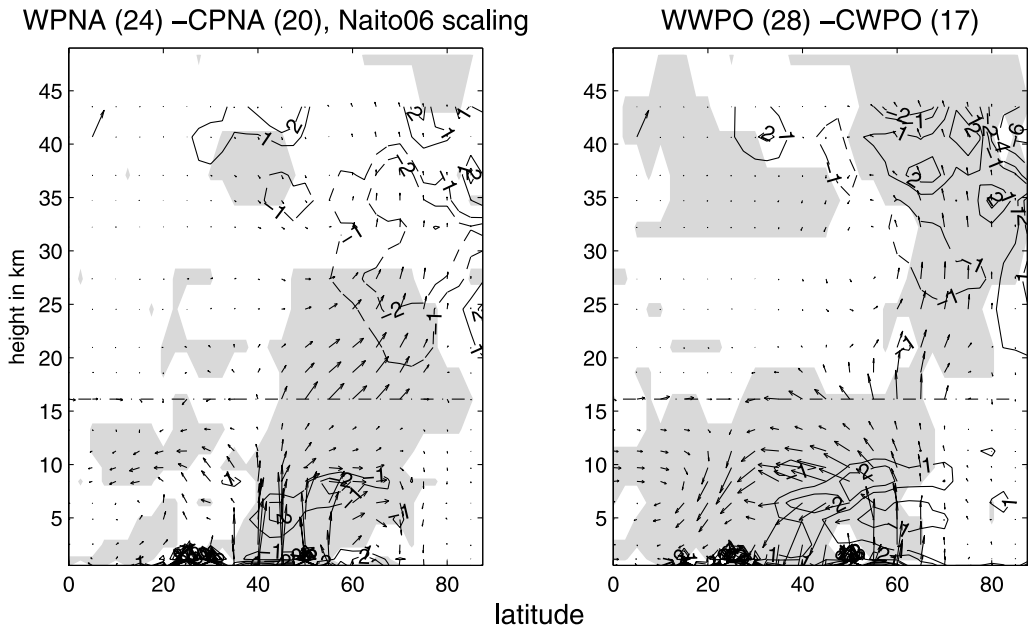

Figure 2. Difference in EP flux (left) between WPNA and CPNA and (right) between WWP and CWP. Only neutral ENSO months but all QBO phases are included. In this and all other EP flux diagrams, regions with significant EP flux are shaded, the divergence of the EP flux is in units of m s^{-1} d^{-1}, and EP flux arrow lengths are multiplied by a factor of 5 above 100 hPa. A reference arrow for the stratosphere is located in the top left hand corner of the plot; its vertical component is 1.0879×10^5 kgs^{-2}, and its horizontal component is 1.25×10^7 kgs^{-2}. The title of the graph contains the number of months making up the composite. The 1 hPa and 1000 hPa levels are excluded.

[21] A Fourier transform of these fields can then be performed, and the phase and amplitude of the wave 1 (and wave 2) components computed. The phase and amplitude can then be used to generate a plot like Figure 6 (right) (see section 5.1). The anomalous wave 1 pattern can be compared to the climatological wave 1 pattern of geopotential height. These plots allow one to visually connect the familiar ENSO teleconnections with the anomalous wave 1 patterns they set up, and to then compare the anomalous wave 1 with the climatological wave 1.

[22] Finally, we plot the area averaged geopotential anomalies from 70°N poleward at all levels in the vertical, multiplied by the square root of the basic state density, so that the square of the amplitude of the curve is proportional to energy. Significance of the difference between various composites is determined through a Student's *t* difference of means test; the reduction of the degrees of freedom is identical to that used in GH07. An example is (Figure 1). *Cohen et al.* [2002] perform a similar calculation using 60°N as a polar cap.

4. Results Part 1: Influence of the PNA, WP, and TNH

[23] In order to understand the means through which ENSO can modulate the vortex strength, we now examine the influence of several major teleconnections associated with ENSO on the vortex. *Manzini et al.* [2006] found that the PNA signal propagates upward and affects the vortex. Section 4 of BO95, on the other hand, concluded that the PNA does not affect the polar vortex. We now reexamine the conclusions of BO95 using our ECMWF data.

[24] See Appendix A for a description of the similarity between the ECMWF and NMC data sets over their 30 years of overlap, and a detailed list of the changes made from the BO95 procedure for the rest of this section. The main conceptual change is that we take composites of months that are PNA, WP, and TNH but are not also ENSO. This enables us to determine the relative ability of PNA, WP, and TNH to affect the vortex independently of ENSO. As will be shown shortly, the teleconnection of ENSO with the greatest influence on the vortex is the PNA. Thus, the CENSO/no PNA and WENSO/no PNA composites are created in order to see how much of the ENSO influence on the polar vortex can be directly attributed to the tendency of ENSO to excite the PNA pattern.

[25] The differences in EP flux and polar cap geopotential height between the different phases of these composites are studied. Maps of geopotential height on a pressure level and the height wave variance confirm the conclusions drawn below, but are excluded for brevity. The average QBO index for the 8 composites of WPNA/noENSO, CPNA/noENSO, WWP/noENSO, and CWP/noENSO, WTNH/noENSO, CTNH/noENSO, WENSO/noPNA, and CENSO/noPNA, are all less than 0.3 standard deviations of the QBO index. Since these composites are not predominately occurring in one phase of QBO, any differences observed are not due to the QBO.

4.1. Anomalous Vortices

[26] Composites of the difference in anomalous polar cap geopotential height between the different phases of ENSO and its teleconnections are plotted in Figure 1. The PNA acts to weaken the vortex, even in the absence of ENSO,

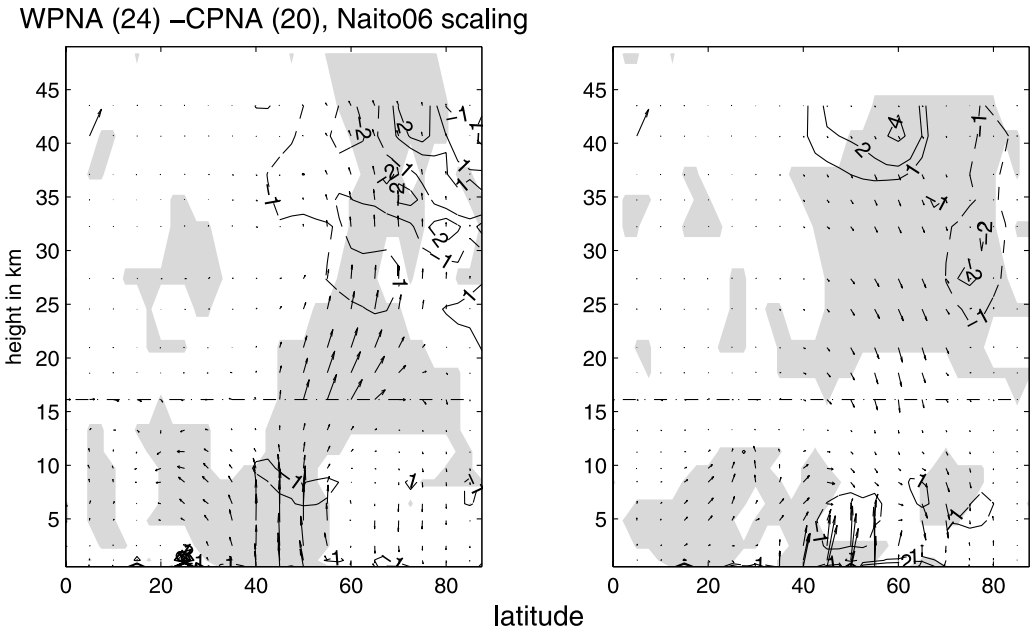

Figure 3. Difference in EP flux between WPNA and CPNA. (left) Wave 1 and (right) wave 2. Only neutral ENSO months but all QBO phases are included. Plotting conventions as in Figure 2.

whereas TNH and WP do not. The weakening of the vortex in PNA is statistically significant at the 95% level in the lower and middle stratosphere. The weakening of the vortex in WENSO/no PNA as compared to CENSO/no PNA is not significant anywhere. In fact, the difference in polar vortex strength between WENSO and CENSO under WQBO, which was found to be significant at greater than 99% in GH07, is not significant at the 95% significance threshold if only neutral PNA months are allowed (not shown, the size of the WENSO/WQBO/no PNA composite is 9 months and the WENSO/WQBO/no PNA composite 14 months). Finally, Figure 1 includes the difference between EQBO and WQBO for all ONDJ months, showing that the weakening of the vortex in PNA is comparable to that in QBO.

[27] The parameters used to define the composites that appear in Figure 1 are varied to explore the robustness of the response. Changing the limits for inclusion into the ENSO/PNA/WP composites has little qualitative effect on the above conclusions. Excluding November or February from our composites also has little qualitative effect on our conclusions that PNA is the teleconnection of ENSO most capable of affecting the polar vortex; excluding November and December increases the modulation of the vortex by ENSO/noPNA. The PNA's (and the TNH's) effect on the vortex is even greater 1 month after, instead of simultaneous with, the PNA/WP/ENSO/TNH event. Excluding the 2 years after the Pinatubo, El Chicòn, and Agung eruptions has little effect on the above conclusions, though the modulation of the vortex in ENSO/noPNA is slightly greater than before. Using the Nino 3.4 index, rather than Nino 3 index, in excluding months that are ENSO in addition to being PNA and WP has more of an effect. Choosing the Nino 3.4 index leads to a reduction of the effect of the PNA on the vortex, but it also leads to a reduction in the difference between WENSO/noPNA and CENSO/noPNA. The difference between WPNA and CPNA under no ENSO is still larger than the difference between the different phases of WP/no ENSO and TNH/no ENSO.

4.2. EP Fluxes

[28] The results of section 4.1 are now diagnosed with EP fluxes. The difference in net (i.e., no wavenumber decomposition) EP flux and its convergence between WPNA/noENSO and CPNA/noENSO is shown in Figure 2 (left), and the individual components of the EP flux in Figure 3. The wave 1 (wave 2) EP flux is increased (decreased) in WPNA versus CPNA, but the decrease in wave 2 is overwhelmed by the increase in wave 1, so that net EP flux convergence at the polar vortex increases. The difference in the net EP flux is significant. Unlike BO95, we find that the wave 1 increase in the extratropics does propagate upward into the stratosphere, where it weakens the vortex.

[29] The same procedure is also followed for the WP and the TNH. The difference in the net EP flux and its convergence between WWP and CWP under neutral ENSO are shown in Figure 2 (right), and the individual components of the EP flux in Figure 4. The wave 1 EP flux increase is confined to high latitudes, and is actually reduced further south. The convergence of the wave 1 EP flux is mostly canceled by the divergence of the wave 2 EP flux. The WPO seems to have little influence on the polar vortex as the wave 1 and wave 2 effects cancel out. Details of the TNH case are not shown for brevity, but like for the WPO, the wave 1 and wave 2 mostly cancel each other out, such that the net signal at the vortex is not discernable.

[30] Finally, Figure 5 shows the difference in wave 1 height variance and EP flux between WENSO/noPNA and CENSO/noPNA. The upper tropospheric anomalies in wave 1 and wave 2 EP flux, and wave 1 and wave 2 height variance, completely go away (wave 2 not shown). The vortex is weakened in this comparison not because of tropospheric processes, but rather because of internal stratospheric processes. The wave 1 EP flux propagates higher

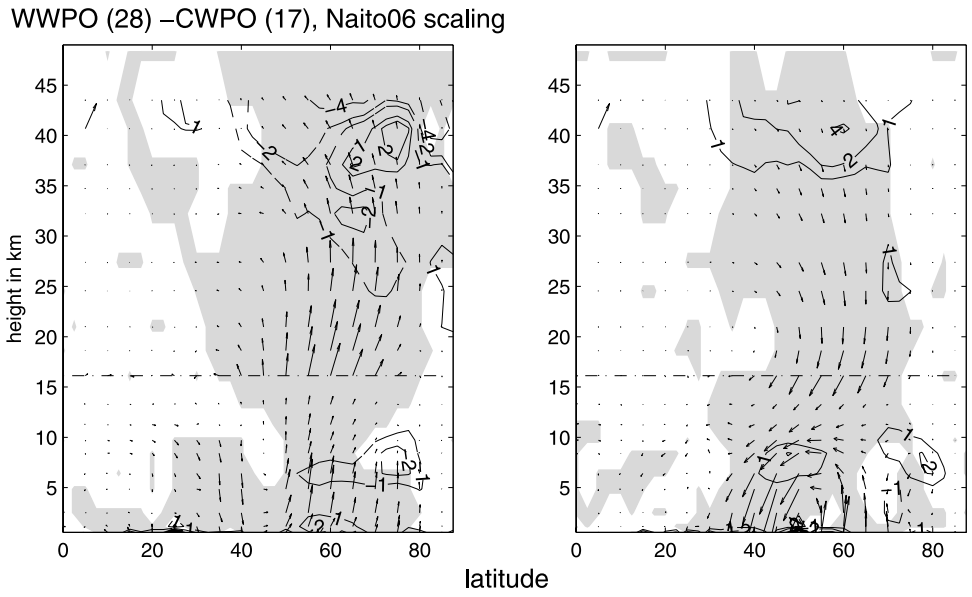

Figure 4. Difference in EP flux between WWP-CWP. (left) Wave 1 and (right) wave 2. Only neutral ENSO months but all QBO phases are included. Plotting conventions as in Figure 2.

into the stratosphere in CENSO than WENSO before breaking. This feature is not statistically significant, however, and is assumed to be due to random internal variability of the stratosphere.

5. Results Part 2: Tropospheric Patterns and Inter-WENSO Variability

[31] Now we address question 2 from the introduction; namely, why is the difference between WENSO and CENSO in vortex strength present under WQBO but not EQBO. Before we present our explanation, we discuss two hypotheses.

[32] One might surmise that the ENSO response is reduced under EQBO as compared to WQBO because of the annual cycle in ENSO teleconnections. *Manzini et al.* [2006] and others have found a seasonal cycle in the WENSO effect on the vortex; if the months in the EQBO composite were earlier in winter than the months in the WQBO composite, the difference in vortex modulation could be tied to the seasonal cycle. To test this, we assign the numeric value of 11 to November, 12 to December, 13

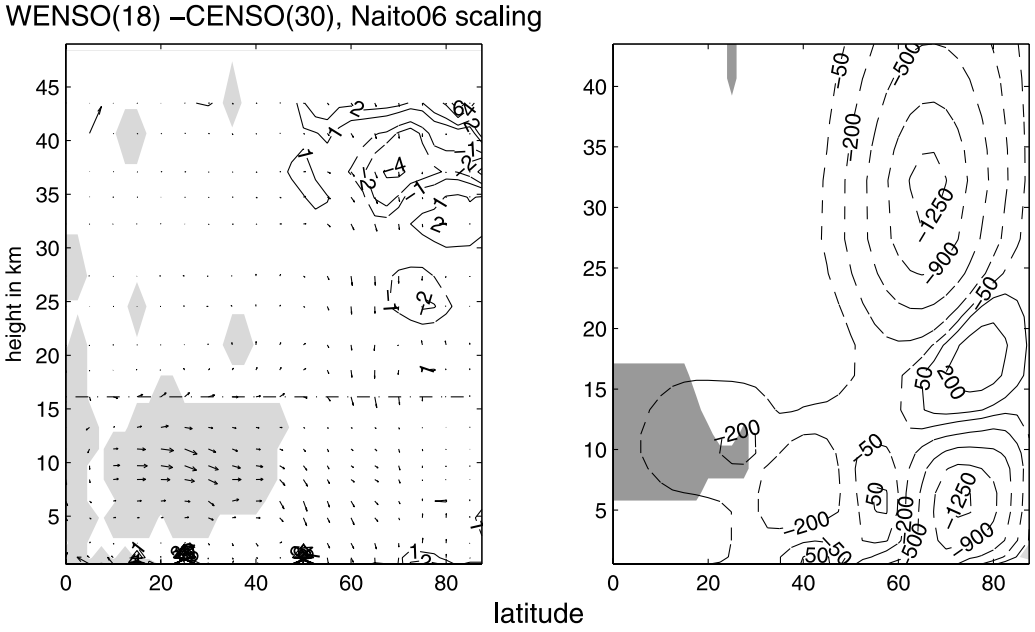

Figure 5. (left) The difference in wave 1 EP flux between WENSO and CENSO under neutral PNA. (right) The difference in height wave 1 variance. All QBO phases included. EP flux plotting conventions as in Figure 2. In this and future wave variance plots, wave 1 height variance is in units of m^2 and has been multiplied by the basic state density.

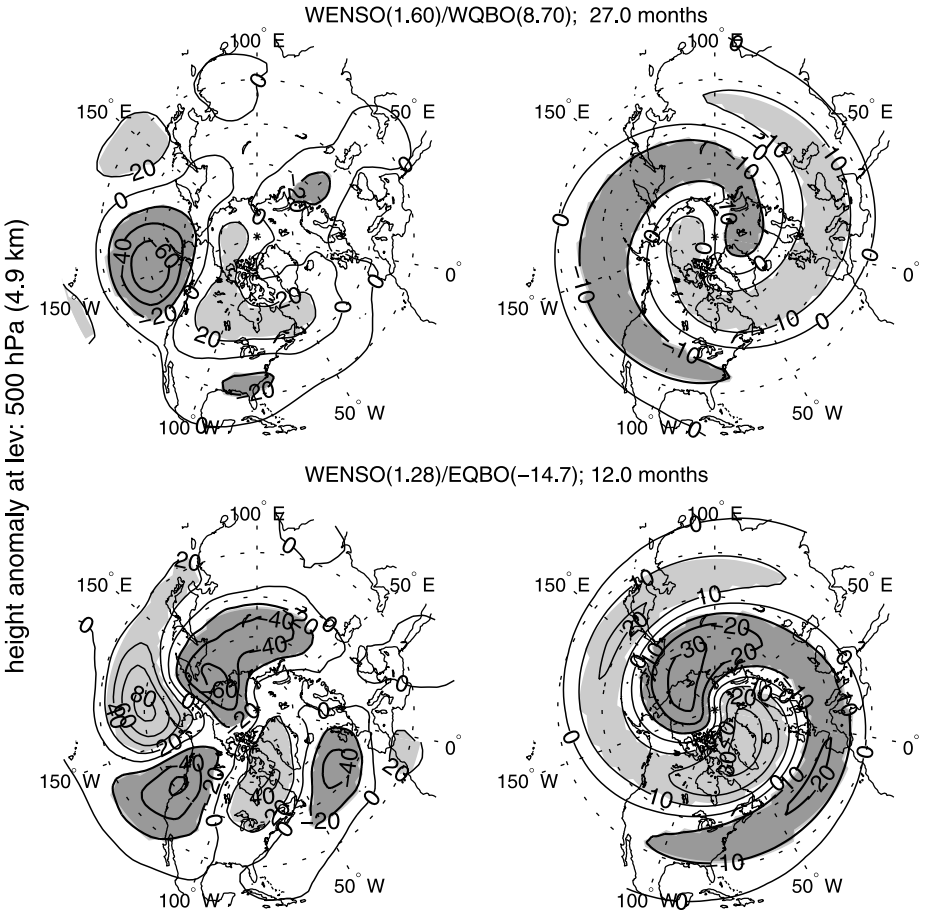

Figure 6. Anomalous height (in m) during WENSO for different phases of QBO at 500 hPa. (left) All waves and (right) wave 1. (bottom) EQBO/WENSO and (top) WQBO/WENSO. For ease of viewing, regions with large positive (negative) anomalies are shaded light (dark) gray.

to January, and 14 to February, and compute the average month of each composite. The average month of the WENSO/WQBO composite is 12.19, whereas the average month in WENSO/EQBO is 12.33. Similarly, the average month in CENSO/WQBO is 12.28, and the average month of the CENSO/EQBO composite is 12.35. Thus, the seasonal cycle is not the cause of the weak response during EQBO in our composite.

[33] *Brönnimann* [2007] and others have suggested that the vortex in WENSO/EQBO is so close to climatology due to some nonlinear mechanism; in other words, the warming of the polar vortex "saturates." A hint that this mechanism cannot fully resolve the question can be seen by comparing the polar cap temperature and geopotential height under WENSO/EQBO to WENSO/noQBO. Throughout the middle and upper stratosphere, the geopotential anomaly from 70°N and poleward is almost twice as large in WENSO/no QBO as in WENSO/EQBO. In the midstratosphere, the polar cap temperature anomaly in WENSO/noQBO approaches 6°C, more than twice the anomaly in WENSO/EQBO. The vortex is actually weaker, albeit not significantly, under WENSO/noQBO than WENSO/EQBO. This difference cannot be traced to the strength of the underlying ENSO events, as the average normalized ENSO index in the months making up the WENSO/EQBO composite is 1.28, whereas the months making up the WENSO/no QBO composite have an average ENSO index of 0.98. For these ENSO indices, the saturation hypothesis would imply a weaker vortex in WENSO/EQBO than in WENSO/no QBO, but the opposite is observed in our short observational record. Though the saturation hypothesis may yet have merit, we do not believe it is sufficient (or needed) to explain the results. In section 5.1, we provide a resolution of this paradox that does not rely on vortex saturation.

5.1. Why the Difference Between WENSO and CENSO Depends on QBO's Phase

[34] The reason that the polar vortex in WENSO/EQBO is not as weak as expected is because WENSO has had different teleconnection patterns during WQBO and neutral QBO than during EQBO. The dominant teleconnection pattern to WENSO under WQBO and neutral QBO is a strengthening of the Aleutian Low, and in particular through the PNA pattern (Figure 6 (top left), WENSO/no QBO not shown), and the dominant teleconnection pattern under WENSO/EQBO is the WP and TNH (Figure 6, bottom left). *Barnston et al.* [1991] reached similar conclusions on data from 1951 to 1989; they found that ENSO under WQBO tended to excite the PNA mode, whereas ENSO under EQBO tended to excite the TNH and WP modes. The disparity in the teleconnections of WENSO between EQBO and WQBO is barotropic throughout the troposphere.

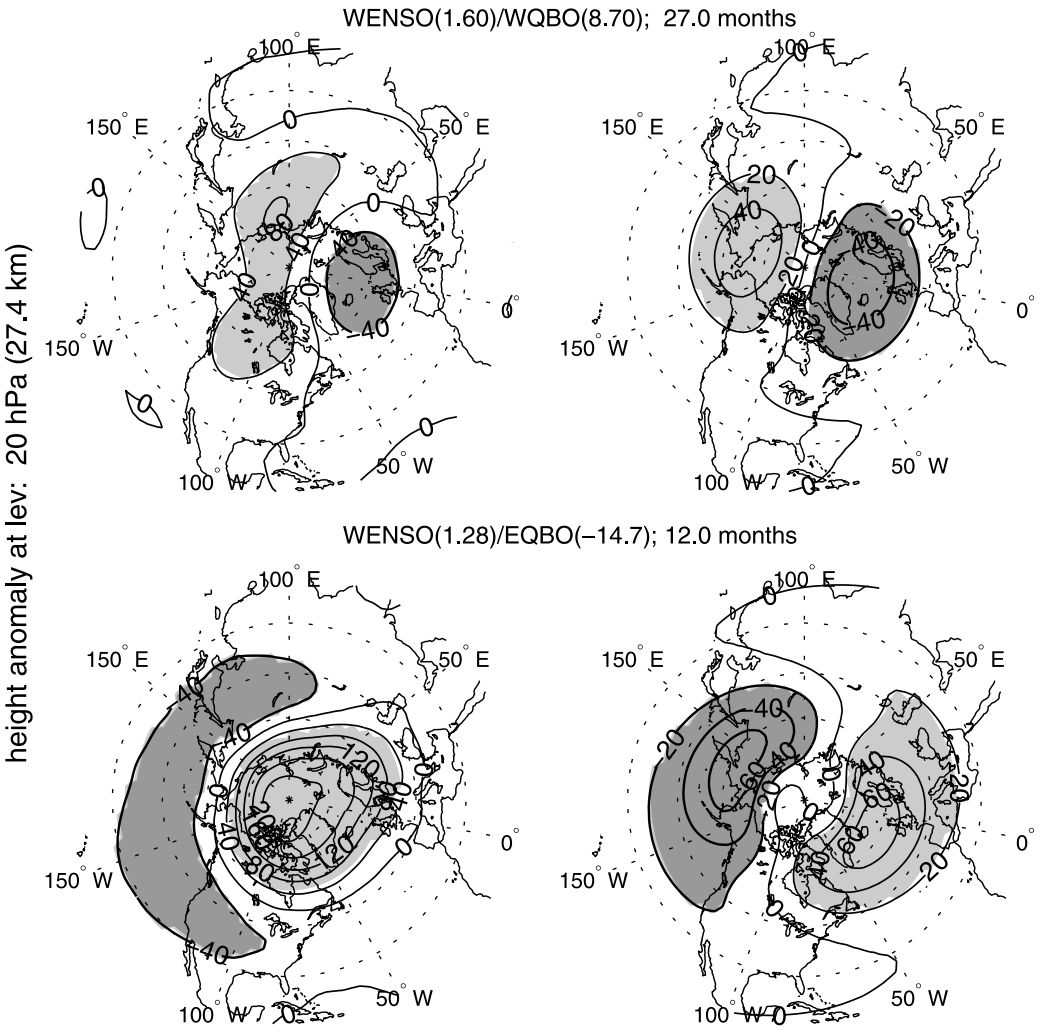

Figure 7. As in Figure 6 but for 20 hPa.

[35] The wave 1 component of the anomaly field can be evaluated (Figures 6 and 7, right) and compared to climatology (Figure 8). In the extratropics, the wave 1 anomaly in WENSO/EQBO (Figures 6 and 7, bottom right) is out of phase with climatology, whereas the wave 1 anomaly in WENSO/WQBO (Figures 6 and 7, top right) is in phase with climatology, as expected from the discussion in section 4.2. (At very high latitudes in the troposphere, the WENSO/EQBO anomaly is in phase with climatological wave 1, consistent with the discussion of the WPO in section 4.2, but the high-latitude response is not effective in weakening the vortex.) The response of the wave 1 component of height in CENSO under both QBO phases in the midlatitude tropospheric region is small (not shown), like in the work by *Manzini et al.* [2006]. Thus, we focus exclusively on the difference between WENSO teleconnections under EQBO and WQBO. In both cases, wave 2 is found not to matter (unlike WP and TNH from section 4), so diagnostics are not shown.

[36] In lieu of graphs at levels between 500 hPa and 20 hPa (which do show an upward propagation of the tropospheric signal but are excluded for brevity), Figure 9 shows the wave 1 height variance. Figure 9 (right) shows the difference between WENSO and CENSO under WQBO and no QBO; during WENSO, wave 1 height leaving the troposphere (in particular from 45°N to 70°N) and converging in the high-latitude stratosphere increases. Figure 9 (left) shows the difference between WENSO and CENSO under EQBO (WENSO/EQBO-CENSO/EQBO); the height variance in WENSO is only slightly enhanced in very high latitudes, and further south is reduced, consistent with the tropospheric response discussed above. EP flux diagrams are consistent with the height variance diagrams in Figure 9 and the EP flux diagrams expected from section 4, and are not shown for brevity.

[37] Unlike WENSO/EQBO, both WENSO/no QBO and WENSO/WQBO force a PNA pattern, which enhances the climatological low present over the North Pacific. Thus, in these two cases only, wave 1 leaving the midlatitude troposphere is enhanced, leading to a weakened vortex.

5.2. Why the Difference Between EQBO and WQBO Depends on ENSO's Phase

[38] GH07 and *Wei et al.* [2007] have noted that the difference between EQBO and WQBO under WENSO is much smaller than the difference between EQBO and WQBO under CENSO; the mechanism through which the QBO affects the polar vortex is not apparent when ENSO is in its warm phase. The results of this study provide a reason

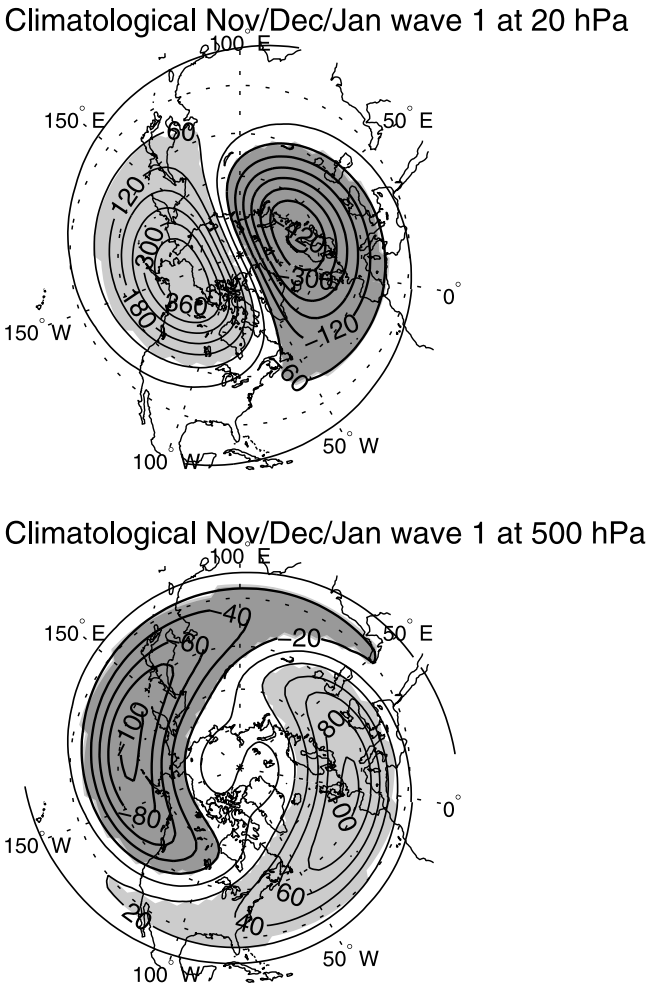

Figure 8. Climatological wave 1 pattern at 500 hPa and 20 hPa. Plotting conventions as in Figure 6.

for this finding. Like the NDJF WENSO/EQBO composite, the ONDJ WENSO/EQBO composite does not have a WPNA pattern (not shown). Thus, the WENSO/EQBO vortex is only slightly weakened as its tropospheric teleconnections do not reinforce the climatological wave 1 in midlatitudes. In contrast, WENSO under WQBO does have tropospheric teleconnections (namely, the PNA) that increase wave 1. Because the midlatitude wave 1 height in the troposphere is greater in WQBO than EQBO under WENSO, the difference between the polar vortex in EQBO and WQBO under WENSO is small despite the QBO's effect on the vortex. Figure 10 shows that in the midlatitude troposphere, wave 1 EP flux and height variance are significantly reduced in EQBO as compared to WQBO under WENSO. At very high latitudes, wave 1 does increase, but its effect on the polar vortex is minimal, as observed in section 5.1. The QBO's influence on the vortex is masked by tropospheric anomalies.

[39] In contrast to WENSO, the wave 1 component of the tropospheric teleconnections in WQBO/CENSO and EQBO/CENSO have similar phases relative to climatology; the CENSO induced wave 1 field in the troposphere is roughly in quadrature with climatology regardless of QBO phase (not shown), with slightly more wave 1 in EQBO than WQBO. Thus, the physical mechanisms generating a stronger vortex in WQBO than EQBO can operate during CENSO without much influence from external factors. Figure 11 shows an increase in EP flux converging on the polar vortex from a weak source in the midlatitude troposphere in EQBO relative to WQBO.

5.3. Cause of the Inter-WENSO Tropospheric Variability

[40] A remaining question concerns the source of the inter-WENSO tropospheric variability; in particular, can the QBO influence the teleconnection patterns forced by

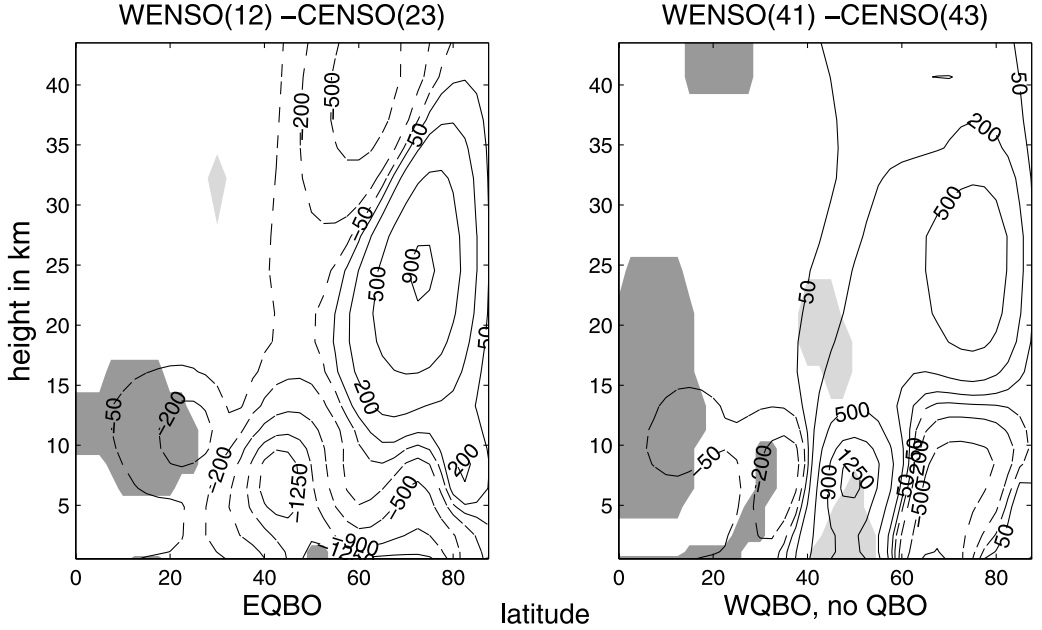

Figure 9. The difference in wave 1 height variance between WENSO and CENSO in NDJF over the NH. (left) EQBO and (right) WQBO or no QBO (limit combination: |ENSO| > 0.6, QBO < −0.6 in Figure 9 (left) and QBO > −0.4 in Figure 9 (right)). Plotting conventions as in Figure 5.

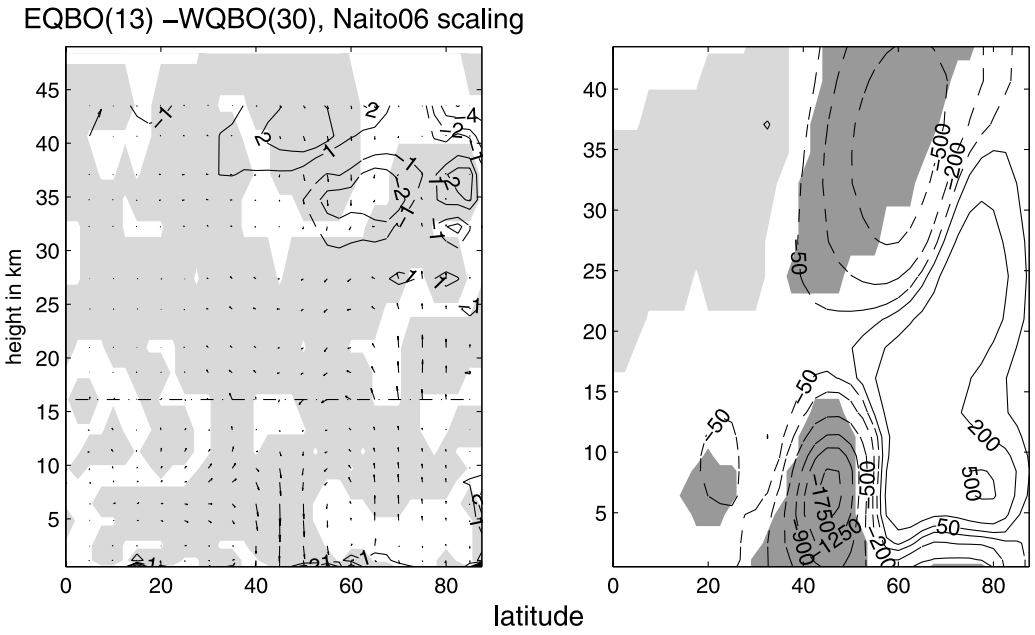

Figure 10. (left) The difference in wave 1 EP flux between EQBO and WQBO under WENSO. (right) wave 1 variance of the height. As in GH07, ONDJ is examined. A month with QBO or ENSO index greater than 0.6 standard deviations is composited as ENSO or QBO. Plotting conventions as in Figures 2 and 5.

WENSO? The surface temperature (1000 hPa) in the tropical Pacific Ocean looks qualitatively similar during WENSO irrespective of QBO phase (not shown). One might hypothesize that the QBO can somehow affect WENSO's tropical convection. Thus, we compute the Rossby wave source term [*Sardeshmukh and Hoskins*, 1988, equation (4)] in the upper troposphere for each phase of QBO(not shown). In the tropics (i.e., south of 20°N) where the QBO might somehow be of relevance, the Rossby wave source looks qualitatively similar in all QBO phases. In the extratropics, however, the source is further east in EQBO than in WQBO or neutral QBO,

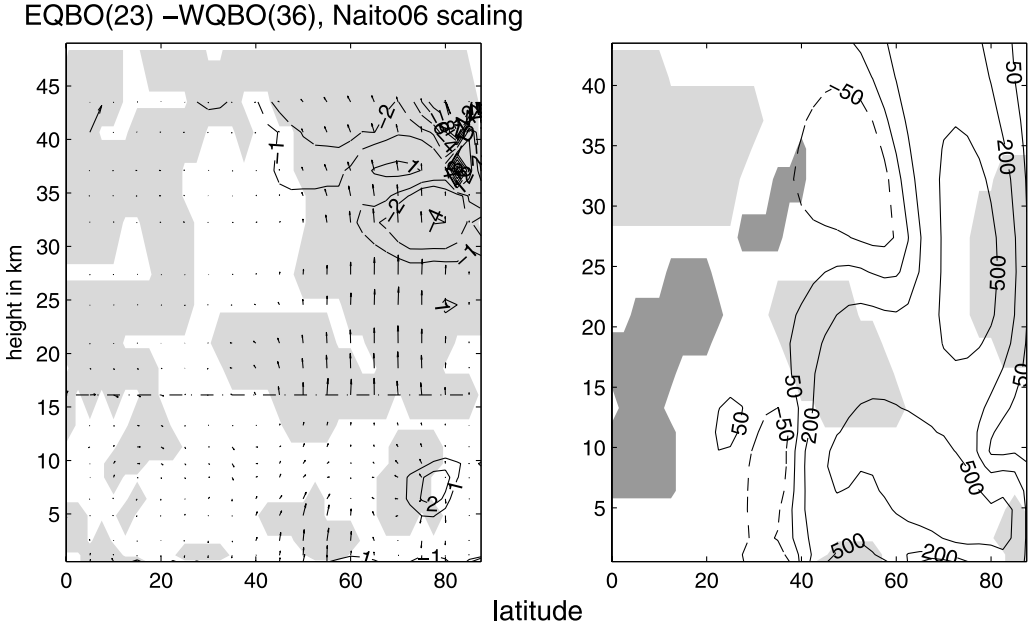

Figure 11. The difference between EQBO and WQBO under CENSO. (left) wave 1 EP flux and (right) wave 1 variance of the height. As in GH07, the months of ONDJ are examined. A month with QBO or ENSO index greater than 0.6 standard deviations is composited as ENSO or QBO. Plotting conventions as in Figures 2 and 5.

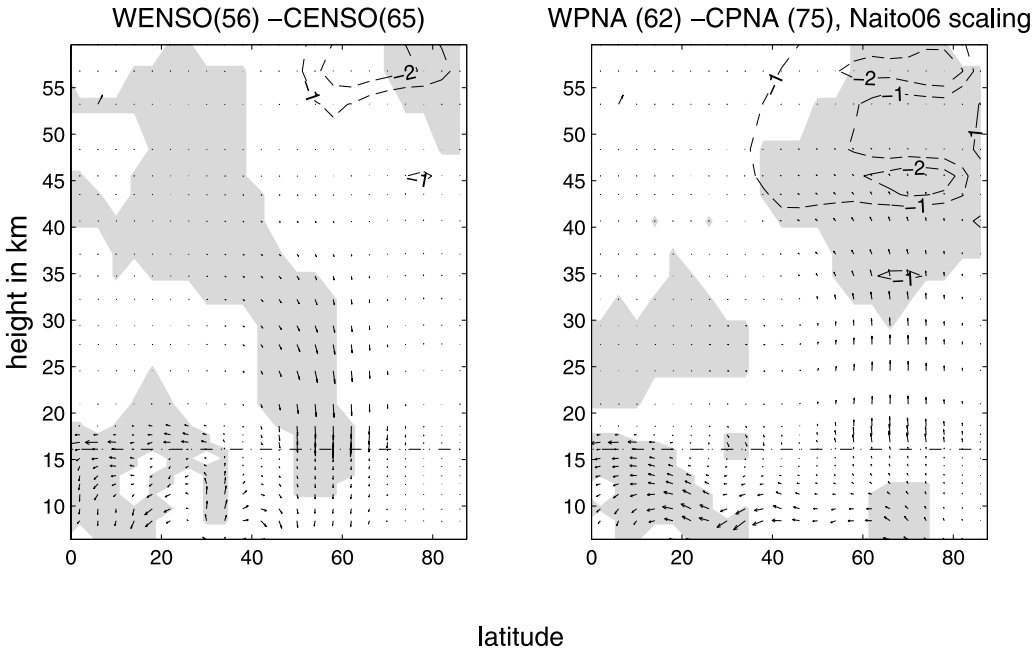

Figure 12. The difference between (left) WENSO and CENSO under no PNA and (right) WPNA and CPNA under no ENSO for the ensemble of 3 44-year CCMVAL simulations with WACCM in NDJF. A month with ENSO or PNA index greater than 0.6 standard deviations is composited as ENSO or PNA. The scales of the vertical and horizontal arrows are different from Figure 2, but otherwise, the conventions from Figure 2 are used.

consistent with the presence of the TNH pattern centered over the far eastern Pacific rather than a PNA pattern further west. The shift of the extratropical Rossby wave source in the EQBO/WENSO composite appears to be due to internal extratropical processes and not to a change in tropical Rossby wave forcing or stratospheric flow, though further work is certainly needed.

[41] Furthermore, the inter-WENSO tropospheric variability might be the result of a sampling fluctuation, as ten of the twelve WENSO/EQBO months occur before 1975. To test this possibility, we compute the correlation of the ENSO time series with the PNA time series over a 30 year window during DJF. Three different groups of months in the 30 year window are chosen: the first group is months that occur under WQBO, the second group is months under EQBO, and the last is all months. If a window is chosen to focus on the early part of the data, the correlation of ENSO with PNA is significantly different depending on whether QBO is westerly or easterly. For example, the correlation of ENSO with PNA is -0.18 under EQBO, 0.39 under WQBO, and 0.21 under all QBO from December 1957 to February 1987. The difference between the -0.18 correlation in EQBO and the 0.39 correlation in WQBO is significant at the 95% level. Later in the record, however, this tendency of ENSO to be correlated with PNA only under WQBO weakens. If the window is chosen from December 1976 through February 2006, the correlation of ENSO with PNA is 0.15 under EQBO, 0.32 under WQBO, and 0.28 under all QBO. The difference in correlation between EQBO and WQBO in the early part of the record largely drops away in later years, and is thus assumed to be a random occurrence. (The lack of WPNA with WENSO in the early part of the record is consistent with the "climate shift" in the late 1970s noted by *Gershunov and Barnett* [1998] and *DeWeaver and Nigam* [2002]. One might say that the *Gershunov and Barnett* [1998] shift is evident only in EQBO but not WQBO.) A similar analysis can be performed for the correlation of ENSO with WP. In the early part of the record, ENSO is correlated with WP at a slightly higher level under EQBO than under WQBO, but in more recent years, that tendency has reversed. Since most of our WENSO/EQBO composite occurred in the early part of our record (consistent with section 4 of GH07), it is not surprising that our WENSO/EQBO shows a strong WP but no PNA. Thus, the lack of PNA but appearance of WP in our WENSO/EQBO composite is most likely a random occurrence related to sampling variability and not a robust relationship; this question will certainly merit revisiting once longer data records are available.

6. Results Part 3: Model Results

[42] The conclusions of section 4 are tested on the 3 ensemble members of the WACCM REF1 run used in CCMVAL [*Garcia et al.*, 2007; *Eyring et al.*, 2006]. The period of 1960–2003 (44 years) is analyzed. In particular, we create the ENSO/noPNA and PNA/noENSO composites for the longer model record in order to test the robustness of our conclusion that the PNA is the dominant means through which ENSO affects the vortex. The WACCM runs have no QBO, so evaluating the robustness of the ECMWF results from section 5 is not possible. The variability of the polar vortex in WACCM is much less than in the ECMWF data; the standard deviation of the geopotential height anomaly from 70°N and poleward in wintertime in WACCM in the stratosphere is roughly half of that in the ECMWF data.

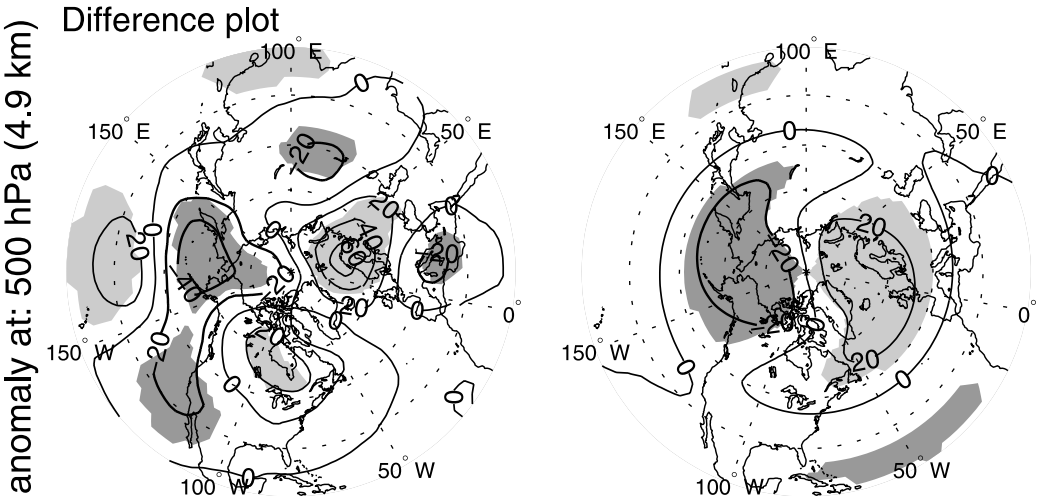

Figure 13. Difference in (left) 500 hPa height anomalies and (right) the wave 1 component, in meters, obtained by averaging 1 month before the 50 weakest NH polar vortices and then subtracting the month before the 50 strongest NH polar vortices. Significant regions at the 95% level are shaded. The wave 1 component can be compared to the bottom of Figure 8.

ENSO affects the polar vortex in WACCM [*Taguchi and Hartmann*, 2006].

[43] A new PNA index is computed for each ensemble of the model data. It is defined as the 1st Principal Component of the 22°N and poleward height from 170E to 110W. By defining the PNA for each ensemble individually, we retain each ensembles random extratropical variability in its PNA index. Visible inspection of the pattern generated when this PC is regressed against the original data confirms that this principal component indexes the PNA pattern.

[44] The WENSO/noPNA, CENSO/noPNA, WPNA/noENSO, and CPNA/noENSO composites in NDJF are created, and the difference in net (all-wave) EP flux is plotted in Figure 12. It is clear that the PNA has a bigger effect than ENSO on the vortex, and that much of ENSO's influence on the vortex is due to the PNA.

[45] In section 4.1, sensitivity was found to the choice of the Nino index used. Figure 12 was created for the Nino 3, Nino 3.4, and Nino 4 indices (not shown); Nino 3 shows the smallest influence of the three. The Nino 3.4 index is used in Figure 12. Because of the longer record, individual calendar months are examined. The difference in EP flux between WPNA and CPNA under no ENSO is greatest in December and January; in those months, EP flux is significantly modulated all the way from the troposphere to the stratosphere. In November and February, the wave 2 component of extratropical tropospheric height is larger than in December and January (not shown), and is out of phase with climatology in WPNA and in phase in CPNA; the net (all wave) EP flux is thus smaller in November and February than in December or January.

7. Conclusions

[46] We conclude with a final simple demonstration that the PNA affects the vortex. We composite the pattern of NH geopotential height 1 month preceding the 50 weakest and 50 strongest vortex anomalies in NDJFM (dropping November or March gives qualitatively similar results) from the ECMWF data. The strength of the vortex is measured by the area averaged geopotential height from 70°N poleward from 3 hPa to 10 hPa (the results were insensitive to this choice of heights as well). (In the month simultaneous with the extreme vortex, the troposphere has a strong Arctic Oscillation signal associated with the anomalous vortex which masks the PNA signal [*Baldwin and Dunkerton*, 1999; *Limpasuvan et al.*, 2004].) All QBO and ENSO phases are included. Significance is determined through a Student's *t* test at every location, with the autocorrelation from month-to-month accounted for as in GH07. The difference in height, and its wave 1 component, between the strong and weak vortex states is shown in Figure 13. The PNA signal is clearly visible and is significant.

[47] WENSO winters have weaker polar vortices than CENSO winters. The dominant reason for this is that WENSO generates teleconnections in the extratropics that enhance the climatological wave 1. This enhanced wave 1 can then propagate upward into the stratosphere and break, thus weakening the vortex. In the WENSO minus CENSO composites, wave 2 has little effect on the vortex. Differences in wave 2 can be important in some of ENSO's teleconnections.

[48] The tendency of WENSO to excite the PNA pattern is the most important way through which ENSO enhances tropospheric wave 1 in both the observational and model data examined. Thus, when WENSO excites a PNA, as it does in WQBO months in the observational record, we should expect a weaker vortex compared to CENSO, and when WENSO excites some other midlatitude teleconnection, like it does in the EQBO months in the observational record, we should not expect the vortex to be much different than in CENSO.

[49] *Hoerling and Kumar* [1997] found that even under identical SST forcings in the tropical Pacific, significant differences in the extratropical teleconnections of WENSO can exist. Similarly, we do not imply the existence of a physical mechanism behind the lack of a PNA pattern in WENSO/EQBO, since the lack of the PNA in WENSO/

EQBO is confined to half of the period of record and could easily have occurred by chance. Thus, the effect of the QBO on the response to ENSO is likely a feature of the particular record we have, and not a real physical effect.

[50] The lack of a PNA in the tropospheric teleconnections of WENSO/EQBO also explains the finding of *Wei et al.* [2007] and GH07 that in reanalysis data, the vortex in EQBO is not significantly weaker than in WQBO under WENSO. Because the midlatitude teleconnections in WENSO/EQBO destructively interfere with climatology, much less wave 1 EP flux crosses the midlatitude tropopause in WENSO/EQBO than in WENSO/WQBO. The mechanism through which QBO weakens the pole is thus masked by a reduction in the wave 1 EP flux; the net result is little change in the polar vortex.

Appendix A

[51] We recreate some of BO95's results for the PNA using their methodology applied only to the 30 years for which they had data. The only two differences are that we are using the ECMWF data rather than the NMC data, and that we are using the CPC's PNA index which is based on the period 1950–2000, not 1963–1994. Agreement in the troposphere is excellent. In the stratosphere, agreement decreases, such that the increase in wave 2 in CPNA relative to WPNA is greater in the ECMWF than the NMC. (This difference would imply that WPNA results in a stronger vortex than CPNA, which is opposite the conclusion we find here). Discrepancies exist in the spatial structure of the height and in the wave 1 height in the stratosphere as well, but these are much smaller than the wave 2 discrepancy. We expect that these discrepancies are due to the different data assimilation schemes used in the two models.

[52] The following changes are made to the procedure BO95 used to compute their Figures 2–12 for our discussion in section 4.

[53] 1. We have 50 years of ECMWF data, whereas they have 30 years of National Meteorological Center data.

[54] 2. We exclude moderate PNA seasons. The PNA is above 0.6 standard deviations in months composited as WPNA or CPNA.

[55] 3. We look at monthly data, rather than seasonal data. For example, if December fits into the WPNA category but January and February are neutral, only December is included.

[56] 4. Instead of looking at the amplitude of the wave 1 and wave 2 components of geopotential height, we look at the variance in wave 1 and wave 2 of the geopotential height. For Rossby waves, the EP flux can be related to the wave variance of the geopotential, as discussed in section 3.

[57] 5. We look at NDJF, not just DJF.

[58] 6. Our PNA index is taken from the Climate Prediction Center Web site (http://www.cpc.ncep.noaa.gov/data/teledoc/telecontents.shtml) who, like BO95, use a varimax rotated EOF definition for the PNA, but the CPC/NCEP uses the longer period of 1950–2000 to define the EOF associated with the PNA.

[59] 7. We evaluate the significance using a two-tailed test. In practice, this means that a probability of greater than 97.5% is needed before a result is deemed significant. This is a more demanding level than BO95.

[60] 8. We exclude any month where the ENSO index is greater than 0.6. This isolates the ENSO effect from the PNA or WP effect we are attempting to find. It also removes much of our available data, as PNA/WP/TNH is correlated with ENSO.

[61] **Acknowledgments.** This work was supported by the Climate Dynamics Program of the National Science Foundation under grant ATM 0409075. We thank the WACCM group at NCAR for providing their model output for this analysis, the Chemistry-Climate Model Validation Activity (CCMVal) of WCRP-SPARC (World Climate Research Programme–Stratospheric Processes and their Role in Climate) for organizing the model data analysis activity, and the British Atmospheric Data Center (BADC) for collecting and archiving the model output.

References

Andrews, D. G., J. R. Holton, and C. B. Leovy (1987), *Middle Atmosphere Dynamics*, Academic, Orlando, Fla.

Baldwin, M. P., and T. J. Dunkerton (1999), Propagation of the Arctic Oscillation from the stratosphere to the troposphere, *J. Geophys. Res.*, *104*(D24), 30,937–30,946.

Baldwin, M. P., and D. O'Sullivan (1995), Stratospheric effects of ENSO-related tropospheric circulation anomalies, *J. Clim.*, *8*, 649–669.

Barnston, A. G., and R. E. Livezey (1987), Classification, seasonality and persistence of low-frequency atmospheric circulation patterns, *Mon. Weather Rev.*, *115*, 1083–1126.

Barnston, A. G., R. E. Livezey, and M. S. Halpert (1991), Modulation of Southern Oscillation–Northern Hemisphere mid-winter climate relationships by QBO, *J. Clim.*, *4*, 203–217.

Brönnimann, S. (2007), The impact of El Nino–Southern Oscillation on European climate, *Rev. Geophys.*, *45*, RG3003, doi:10.1029/2006RG000199.

Brönnimann, S., J. Luterbacher, J. Staehelin, T. M. Svendby, G. Hansen, and T. Svene (2004), Extreme climate of the global troposphere and stratosphere in 1940–42 related to El Niño, *Nature*, *431*, 971–974, doi:10.1038/nature02982.

Brönnimann, S., M. Schraner, B. Müller, A. Fischer, D. Brunner, E. Rozanov, and T. Egorova (2006), The 1986-1989 ENSO cycle in a Chemical Climate Model, *Atmos. Chem. Phys.*, *6*, 4669–4685.

Camp, C. D., and K. K. Tung (2007), Stratospheric polar warming by ENSO in winter, a statistical study, *Geophys. Res. Lett.*, *34*, L04809, doi:10.1029/2006GL028521.

Cohen, J., D. Salstein, and K. Saito (2002), A dynamical framework to understand and predict the major Northern Hemisphere mode, *Geophys. Res. Lett.*, *29*(10), 1412, doi:10.1029/2001GL014117.

DeWeaver, E., and S. Nigam (2002), Linearity in ENSO's atmospheric response, *J. Clim.*, *15*, 2446–2461.

Dunkerton, T. J., C. P. Hsu, and M. E. McIntyre (1981), Some Eulerian and Lagrangian diagnostics for a model stratospheric warming, *J. Atmos. Sci.*, *38*, 819–843, doi:10.1175/1520-0469.

Eyring, V., et al. (2006), Assessment of temperature, trace species, and ozone in chemistry-climate model simulations of the recent past, *J. Geophys. Res.*, *111*, D22308, doi:10.1029/2006JD007327.

Garcia, R. R., D. Marsh, D. Kinnison, B. Boville, and F. Sassi (2007), Simulations of secular trends in the middle atmosphere, 1950–2003, *J. Geophys. Res.*, *112*, D09301, doi:10.1029/2006JD007485.

Garcia-Herrera, R., N. Calvo, R. R. Garcia, and M. A. Giorgetta (2006), Propagation of ENSO temperature signals into the middle atmosphere: A comparison of two general circulation models and ERA-40 reanalysis data, *J. Geophys. Res.*, *111*, D06101, doi:10.1029/2005JD006061.

Garfinkel, C. I., and D. L. Hartmann (2007), Effects of the El Nino–Southern Oscillation and the Quasi-Biennial Oscillation on polar temperatures in the stratosphere, *J. Geophys. Res.*, *112*, D19112, doi:10.1029/2007JD008481.

Gershunov, A., and T. P. Barnett (1998), Interdecadal modulation of ENSO teleconnections, *Bull. Am. Meteorol. Soc.*, *79*, 2715–2725.

Hoerling, M. P., and A. Kumar (1997), Why do North American climate anomalies differ from one El Niño event to another?, *Geophys. Res. Lett.*, *24*, 1059–1062.

Hoerling, M. P., A. Kumar, and M. Zhong (1997), El Nino, La Nina, and the nonlinearity of their teleconnections, *J. Clim.*, *10*, 1769–1786.

Holton, J. R., and H. C. Tan (1980), The influence of the equatorial Quasi-Biennial Oscillation on the global circulation at 50 mb, *J. Atmos. Sci.*, *37*, 2200–2208.

Horel, J. D., and J. M. Wallace (1981), Planetary scale atmospheric phenomena associated with the Southern Oscillation, *Mon. Weather Rev.*, *109*, 813–829.

Hoskins, B. J., and D. Karoly (1981), The steady linear response of a spherical atmosphere to thermal and orographic forcing, *J. Atmos. Sci.*, *38*, 1179–1196.

Limpasuvan, V., D. W. J. Thompson, and D. L. Hartmann (2004), The life cycle of the Northern Hemisphere sudden stratospheric warmings, *J. Clim.*, *17*, 2584–2596.

Manzini, E., M. A. Giorgetta, L. Kornbluth, and E. Roeckner (2006), The influence of sea surface temperatures on the northern winter stratosphere: Ensemble simulations with the MAECHAM5 model, *J. Clim.*, *19*, 3863–3881.

Naito, Y., and S. Yoden (2006), Behavior of planetary waves before and after stratospheric sudden warming events in several phases of the equatorial QBO, *J. Atmos. Sci.*, *63*, 1637–1649, doi:10.1175/JAS3702.1.

Randel, W. J., et al. (2004), The SPARC intercomparison of middle atmosphere climatologies, *J. Clim.*, *17*, 986–1003.

Sardeshmukh, P. D., and B. J. Hoskins (1988), The generation of global rotational flow by steady idealized tropical divergence, *J. Atmos. Sci.*, *45*, 1228–1251.

Sassi, F., D. Kinnison, B. A. Bolville, R. R. Garcia, and R. Roble (2004), Effect of El Niño–Southern Oscillation on the dynamical, thermal, and chemical structure of the middle atmosphere, *J. Geophys. Res.*, *109*, D17108, doi:10.1029/2003JD004434.

Simmons, A., J. M. Wallace, and G. Branstator (1983), Barotropic wave propagation and instability, and atmospheric teleconnection patterns, *J. Atmos. Sci.*, *40*, 1363–1392.

Taguchi, M., and D. L. Hartmann (2006), Increased occurrence of stratospheric sudden warming during El Niño as simulated by WAACM, *J. Clim.*, *19*, 324–332, doi:10.1175/JCLI3655.1.

Trenberth, K. E., G. W. Branstator, D. Karoly, A. Kumar, N.-C. Lau, and C. Ropelewski (1998), Progress during TOGA in understanding and modeling global teleconnections associated with tropical sea surface temperatures, *J. Geophys. Res.*, *103*, 14,291–14,324.

Uppala, S. M., et al. (2005), The ERA-40 reanalysis, *Q. J. R. Meteorol. Soc.*, *131*(612), 2961–3012.

Vallis, G. K. (2006), *Atmospheric and Oceanic Fluid Dynamics: Fundamentals and Large-Scale Circulation*, Cambridge Univ. Press, Cambridge, U. K.

Wei, K., W. Chen, and R. Huang (2007), Association of tropical Pacific sea surface temperatures with the stratospheric Holton-Tan Oscillation in the Northern Hemisphere winter, *Geophys. Res. Lett.*, *34*, L16814, doi:10.1029/2007GL030478.

C. I. Garfinkel and D. L. Hartmann, Department of Atmospheric Science, University of Washington, Seattle, WA 98195, USA. (cig4@atmos.washington.edu; dennis@atmos.washington.edu)